EurJOC European Journal of Organic Chemistry

FULL PAPER

DOI: 10.1002/ejoc.201200245

Decalactone Derivatives from *Corynespora cassiicola*, an Endophytic Fungus of the Mangrove Plant *Laguncularia racemosa*

Weaam Ebrahim,[a,b] Amal H. Aly,[a] Attila Mándi,[c] Frank Totzke,[d] Michael H. G. Kubbutat,[d] Victor Wray,[e] Wen-Han Lin,[f] Haofu Dai,[g] Peter Proksch,[a] Tibor Kurtán,*[c] and Abdessamad Debbab*[a]

Keywords: Natural products / Medicinal chemistry / Drug discovery / Fungi / Structure elucidation / Conformation analysis / Lactones

Chemical investigation of the ethyl acetate extract of *Corynespora cassiicola*, isolated from leaf tissues of the Chinese mangrove medicinal plant *Laguncularia racemosa*, yielded four new secondary metabolites, including three decalactones, xestodecalactones D–F (**1**–**3**) as well as corynesidone D (**4**), in addition to four known compounds. The structures of the new compounds were determined on the basis of one- and two-dimensional NMR spectroscopy as well as by high-resolution mass spectrometry. Absolute configurations of the optically active compounds **1**–**3** were determined by TDDFT ECD calculations of their solution conformers, proving that they belong to the (11*S*) series of xestodecalactones, opposite to the (11*R*) configuration of the known xestodecalactones A–C. All compounds were tested against a panel of human protein kinases. Among the isolated compounds, two inhibited several kinases such as IGF1-R and VEGF-R2 with IC_{50} values mostly in the low micromolar range.

Introduction

Over the course of the last century, endophytic fungi have become a promising source of new natural products and drug leads that are of great potential for medicinal and agricultural applications.[1–5] Examples include the potent antimycotic cryptocandin A,[6] the HIV-1 integrase inhibitors xanthoviridicatins E and F,[7] and *Helicobacter pylori* inhibiting rhizotonic acid.[8] Furthermore, the detection of several important plant secondary metabolites in endophytic fungal cultures, such as taxol,[9,10] camptothecin,[11] and podophyllotoxin,[12] suggested their possible use as alternative sources of these metabolites.

[a] Institut für Pharmazeutische Biologie und Biotechnologie, Heinrich-Heine-Universität Düsseldorf, Universitätsstrasse 1, Geb. 26.23, 40225 Düsseldorf, Germany
Fax: +49-(0)21-18111923
E-mail: abdessamad.debbab@uni-duesseldorf.de
[b] Department of Pharmacognosy, Faculty of Pharmacy, Mansoura University, 35516 Mansoura, Egypt
[c] Department of Organic Chemistry, University of Debrecen, POB 20, 4010 Debrecen, Hungary
Fax: +36-52453836
E-mail: kurtan.tibor@science.unideb.hu
[d] ProQinase GmbH, Breisacher Strasse 117, 79106 Freiburg, Germany
[e] Helmholtz Centre for Infection Research, Inhoffenstraße 7, 38124 Braunschweig, Germany
[f] National Research Laboratories of Natural and Biomimetic Drugs, Peking University, Health Science Center, 100083 Beijing, P. R. of China
[g] Institute of Tropical Bioscience and Biotechnology, Chinese Academy of Tropical Agricultural Sciences, Haikou 571101, Hainan, P. R. of China

However, due to a reduced hit-rate of novel compounds from terrestrial endophytic fungi, the focus of drug discovery is shifting more in favor of endophytes from extreme and less investigated habitats. Such interesting biotopes are known to influence the fungal secondary metabolites and their respective host plants.[2,4,13,14]

Mangrove forests, constituting a transition zone between terrestrial and marine habitats, are an example of such an environment. Plant species inhabiting this particular ecosystem are adapted to frequent and fluctuating environmental changes, including high saline concentrations, adaptation to low oxygen, nutrient limitation, tidal flushing, high temperatures, excessively high light, drought, and an invigorated microbial community due to warm and damp conditions.[15–17] In this context, endophytic fungi colonizing mangrove plants have been suggested to contribute to their adaptation to harsh environmental factors,[18] in many cases by the production of unique functional metabolites,[3,19,20] which are also of considerable pharmaceutical and therapeutic potential.[21] Fungi are well-known to produce a diverse range of polyketide-derived secondary metabolites, from simple aromatic rings to complex, highly modified reduced-type compounds, such as macrolides.[22,23] This wide variety of structures is initially formed from poly-β-keto chains (poly-β-keto esters) biosynthesized through a decarboxylative condensation of malonyl-CoA units. Aromatic structures are then rationalized in terms of aldol and Claisen reactions.[24] The biosynthesis of small macrolides such as curvularin, which is an octaketide macrolide produced by some *Curvularia*,[25] *Alternaria*,[26] and *Penicil-*

 © 0000 Wiley-VCH Verlag GmbH & Co. KGaA, Weinheim

lium[27] species, is well-studied.[28,29] However, to the best of our knowledge, the biosynthesis of decalactone and octalactone derivatives has not been investigated.

During our ongoing search for new bioactive metabolites from plant-derived endophytes,[30–33] we isolated an endophytic *Corynespora cassiicola* strain from leaf tissues of the mangrove plant *Laguncularia racemosa* (L) Gaertn. (Combretacaeae), collected at Hainan Island in China. *L. racemosa* is an evergreen tree that is common in mangrove forests extending along the Pacific and Atlantic coasts and tropical southern Asia.[34] A bark infusion is historically used as an astringent and tonic, and as a folk remedy for dysentery, aphthae, fever, and scurvy.[35,36] Morton reported that the antitumor activity of this plant was attributed to its tannin content,[37] and its leaves possess antibiotic properties against *Escherichia coli*.[38]

To date, the chemical constituents of fungi belonging to the genus *Corynespora* have received scant attention. A literature survey showed that an endolichenic *Corynespora* sp. yielded ten secondary metabolites of polyketide origin: corynesporol, herbarin, 1-hydroxydehydroherbarin, 9-*O*-methylscytalol, scytalol, 7-desmethylherbarin, 8-hydroxyherbarin, 8-methylfusarubin, scorpinone, and 8-*O*-methylbostrycoidin.[39,40] Furthermore, other metabolites of depsidone origin, including depsidones A–C and diaryl ethers,[41] 6-(3′-hydroxybutyl)-7-*O*-methylspinochrome B,[42] as well as 2,5,7-trihydroxy-3-methoxynaphthalene-1,4-dione[43] were likewise reported from different *Corynespora* strains. In the present study, we provide a comprehensive analysis of natural products produced by *Corynespora cassiicola* and report on four new, as well as four known, metabolites.

Results and Discussions

The crude ethyl acetate extract of *Corynespora cassiicola*, cultured on solid rice medium, was taken to dryness and then partitioned between *n*-hexane and 90% methanol. The 90% methanol fraction was purified by chromatography over different stationary phases (silica gel and Sephadex LH-20). Final purification by preparative reversed-phase HPLC afforded eight compounds, the structures of which were elucidated by high-resolution ESI mass spectrometry and NMR spectroscopy. This resulted in the identification of four new compounds, including three decalactones, xestodecalactones D–E (**1**–**3**) and the depsidone corynesidone D (**4**), together with four known compounds, corynesidone A (**5**) and B (**6**),[41] 2,5,7-trihydroxy-3-methoxynaphthalene-1,4-dione (**7**),[43] and 6-(3′-hydroxybutyl)-7-*O*-methylspinochrome B (**8**).[42]

Compound **1** was obtained as a yellowish-white amorphous powder. Its molecular formula was determined as $C_{15}H_{18}O_7$ on the basis of the $[M + H]^+$ signal detected at *m/z* 311.1134 in the HRMS (ESI). Comparison of the NMR spectroscopic data of **1** with those reported for xestodecalactones B and C, previously isolated from *Penicillium* cf. *montanense*,[44] indicated a close structural relationship between the compounds. However, in comparison to xestodecalactones B and C,[44] the ^{1}H NMR spectrum of **1** showed an additional aromatic methoxyl group (δ_H = 3.68 ppm) and the absence of one aromatic proton Table 1. Inspection of the COSY correlations (Figure 1) revealed the presence of a continuous spin system from CH_2-8 (δ_H = 3.45 and 2.66 ppm) to 11-CH_3 (δ_H = 1.16 ppm) in analogy to known xestodecalactones.[44] Moreover, a homonuclear long-range correlation was observed for CH_2-13 (δ_H = 3.54 ppm) to H-4 (δ_H = 6.22 ppm), suggesting their neighboring positions. The attachment of the methoxyl group to the aromatic ring at C-2 (δ_C = 134.1 ppm) was established on the basis of its HMBC correlation (Figure 2). Moreover, diagnostic HMBC correlations of CH_2-13 to C-4, C-5, C-6 and C-12, as well as of H-4 to C-2, C-3, C-6 and C-13 revealed the phenylacetic acid substructure of **1**. The observed downfield chemical shift of CH_2-8 and its HMBC correlation to the carbonyl carbon appearing at δ_C = 204.5 ppm (C-7) indicated its α relationship to C-7. Additional correlations were observed for CH_2-8 with C-9, CH_2-10 (δ_H = 1.76 and 1.87 ppm) with C-8 and C-9, H-11 (δ_H = 4.81 ppm) with C-9, and 11-CH_3 with C-10 and C-11, thus establishing the fragment CH_2(8)CH(9)OCH_2(10)CH(11)CH_3. The connection of C-7 to the aromatic ring was evident from the four-bond long-range ω-correlation of H-4 to C-7. Furthermore, correlation of H-11 to the ester carbonyl group at δ_C = 169.1 ppm (C-12) indicated the linkage between C-12 and the oxygenated methine group CH-11 through an ester bond.

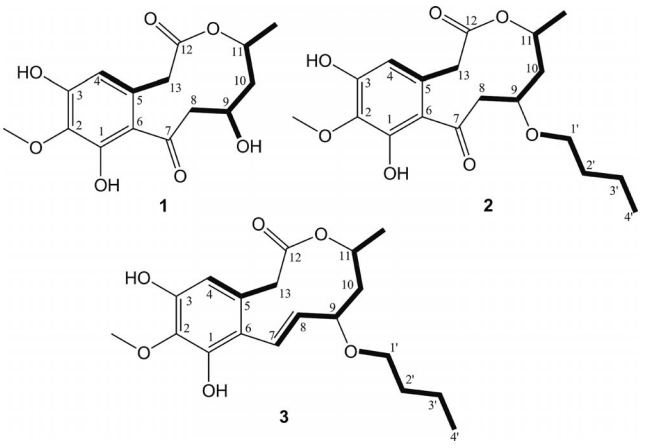

Figure 1. COSY correlations of the new decalactones.

The relative configuration of **1** was obtained from a careful analysis of the coupling constants observed in the well-resolved 1D ^{1}H NMR spectrum, as well as from ROESY correlations (**1** in Figure 6). The coupling constants of H-8, 9, and 10 were in accord with the lowest-energy computed conformation. The axial orientation of H-11 was evident from the large $^3J_{H-11ax,H-10ax}$ value (6.7 Hz) showing the *trans* diaxial relationships of H-11_{ax} and H-10_{ax}. The three ROESY correlations of **1** shown in Figure 6 and the coupling constants of H-9_{ax} in dimethyl sulfoxide (DMSO) ($^3J_{H-8ax,H-9ax}$ = 9.4, $^3J_{H-10ax,H-9ax}$ = 6.7 Hz) agree well with

 © 0000 Wiley-VCH Verlag GmbH & Co. KGaA, Weinheim

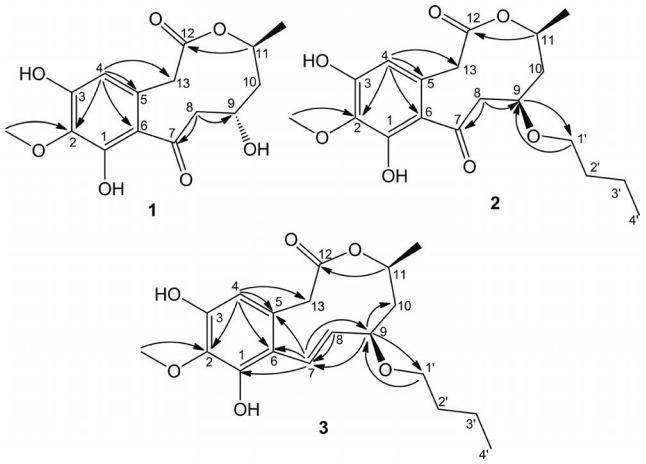

Figure 2. Key HMBC correlations of the new decalactones.

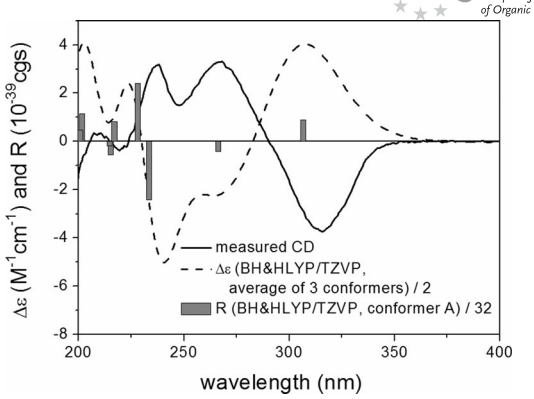

Figure 3. Experimental ECD spectrum of **1** in acetonitrile compared with the Boltzmann-weighted BH&HLYP/TZVP spectrum calculated for the three lowest-energy conformers of (9*R*,11*R*)-**1**. Bars represent rotatory strength of the lowest-energy conformer.

the computed conformation, indicating the axial arrangement. For the determination of the absolute configuration, ECD calculation of the solution conformers and comparison with the solution experimental ECD curve were carried out, which was found previously to be a powerful and reliable tool for this purpose.[45,46] The measured solution ECD spectrum of **1** exhibited three Cotton effects (CEs) above 225 nm; a negative one at 316 and positive ones at 268 and 238 nm. The initial MMFF conformational search of **1** afforded 49 conformers, the DFT reoptimization of which at the B3LYP/6-31G (d) level reduced this to three above 1% population (Figure 3). The three conformers showed minor differences in the orientation of the phenolic hydroxyl and methoxyl groups, whereas the fused heterocycle adopted nearly the same conformation. Due to their similar conformations, the computed ECD spectra of the individual conformers were also quite similar. The Boltzmann-weighted average ECD spectra of (9*R*,11*R*)-**1** obtained by various functionals (B3LYP, BH&HLYP, PBE0) and the TZVP basis set gave mirror image ECD curves of the experimental curve, which allowed the absolute configuration to be determined as (–)-(9*S*,11*S*)-**1** (Figure 3). Hence, **1** was identified as a new natural product for which the name xestodecalactone D was proposed.

Compound **2** was obtained as a yellowish amorphous mass. HRMS (ESI) showed a prominent $[M + H]^+$ signal at *m*/*z* 367.1752, indicating a molecular formula of $C_{19}H_{26}O_7$, with an increase of 56 amu compared to **1**. ^{1}H NMR spectroscopic data of **2** (Table 1) were comparable to those of **1**, thus indicating a structural resemblance between both compounds. Common signals were attributed to one aromatic proton (δ_H = 6.21 ppm, H-4), a methoxyl group (δ_H = 3.69 ppm, 2-OCH_3), two aromatic hydroxyl groups (δ_H = 9.36 and 9.73 ppm, assigned for 1- and 3-OH, respectively), and a methylene group (δ_H = 3.46 and 3.78 ppm, CH_2-13). The COSY spectrum (Figure 1) revealed the presence of a similar spin system from CH_2-8 (δ_H = 3.04 and 2.93 ppm) to 11-CH_3 (δ_H = 1.10 ppm) as in **1**, but lacking the signal corresponding to 9-OH. Further inspection of the COSY spectrum indicated an additional spin system extending from CH_2-1′ (δ_H = 3.41 ppm) to CH_3-4′ (δ_H = 0.88 ppm), which was attributed to a *n*-butyl side chain, thus accounting for the difference in the molecular weight between **1** and **2** (56 amu). As in **1**, a homonuclear long-range correlation of CH_2-13 to H-4 was detected. The HMBC experiment confirmed the attachment of the methoxyl group at C-2, and established the phenylacetic acid substructure of **2** by diagnostic correlations of CH_2-13 and H-4 in analogy to **1**. Further inspection of the HMBC spectrum (Figure 2) corroborated the attachment of CH_2-8 to the carbonyl C signal appearing at δ_C = 204.1 ppm (C-7), and established the fragment CH_2(8)CH(9)CH_2(10)CH(11)-CH_3 through correlations of CH_2-8 to C-9, CH-9 (δ_H = 3.68 ppm) to C-1′ and C-11, CH_2-10 (δ_H = 1.67 and 1.94 ppm) to C-8 and C-9, H-11 (δ_H = 4.75 ppm) to C-9, and 11-CH_3 to C-10 and C-11. The four-bond long-range ω-correlation of H-4 to C-7, and the correlation of H-11 to the ester carbonyl at C-12 (δ_C = 168.8 ppm) established the connection of the detected substructures. Moreover, correlation of CH_2-1′ (δ_H = 3.41 ppm) to C-9 (δ_C = 76.1 ppm) indicated that the *n*-butyl moiety was attached to C-9 through an ether linkage.

Because the coupling constants extracted from ^{1}H NMR spectrum of **2** and the ROESY correlations (see the Supporting Information, Figure S1) were similar to those of xestodecalactone B,[44] the relative configuration of **2** was assigned as *cis*. H-9 and H-11 were found to have an axial orientation from their large vicinal coupling constants ($^3J_{H-8ax,H-9ax}$ = 10.1 Hz, $^3J_{H-10ax,H-11ax}$ = 11.5 Hz). Furthermore, a diagnostic ROESY correlation was observed for H-9 to H-11, indicating their 1,3-*cis* orientation and implying the (9*R**,11*S**) relative configuration as shown for **2** in Figure 6. The structures of all the computed conformers are fully in accordance with the NMR spectroscopic data. The solution ECD spectrum of **2** was very similar to that of (9*S*,11*S*)-**1**. A solution ECD calculation protocol was pursued on the 9-methoxyl model compound of **2**, which revealed that the chiral center was inverted compared to those of (9*S*,11*S*)-**1**. The MMFF conformational search and DFT optimization provided five major conform-

 © 0000 Wiley-VCH Verlag GmbH & Co. KGaA, Weinheim

Table 1. NMR spectroscopic data of xestodecalactone D (**1**), xestodecalactone E (**2**), and xestodecalactone F (**3**).

Position	**1**[a]		**2**[b]		**3**[a]	
	δ_C	δ_H	δ_C	δ_H	δ_C	δ_H
1	148.5		149.4		148.7	
2	134.1		134.2		133.9	
3	151.2		151.5		149.3	
4	110.5	6.22, s	110.1	6.21, s	105.7	6.14, s
5	128.6		127.7		130.6	
6	120.5		121.7		116.1	
7	204.5		204.1		127.8	6.18, d (16.2)
8	52.4	2.66, dd (9.4, 14.6)	60	3.04, dd (10.1, 15.3)	134.3	5.46, dd (9.5, 16.1)
		3.45, br. dd (2.2, 14.6)		2.93, br. d (15.1)		
9	63.9	4.03, m	76.1	3.68, m	79.9	3.84, ddd (5.1, 9.5, 10.8)
10	41.8	1.76, ddd (6.7, 7.3, 14.6)	52.1	1.67, ddd (9.8, 11.6, 14.6)	42.7	1.77, ddd (10.8, 10.8, 13.8)
		1.87, ddd (3.2, 4.0, 14.6)		1.94, br. d (14.6)		2.00, ddd (1.0, 5.1, 13.8)
11	68.2	4.81, ddq (4.0, 6.7, 6.5)	70.9	4.75, ddq (2.6, 11.5, 6.2)	68.6	4.84, ddq (0.9, 10.8, 6.4)
12	169.1		168.8		172.9	
13	38.6	3.54, br. s	38.9	3.46, d (18.7)	40.6	3.29[c]
				3.78, d (18.7)		3.76, d (15.5)
1′			67.1	3.41, m[d]	66.6	3.27, m[c][d]
						3.42, m[d]
2′			31.5	1.46, m[d]	31.4	1.45, m[d]
3′			18.9	1.32, m[d]	18.9	1.30, m[d]
4′			13.7	0.88, t (7.3)	13.7	0.86, t (7.4)
2-OCH_3	60	3.68, s	60.1	3.69, s	59.8	3.66, s
11-CH_3	19.5	1.16, d (6.5)	20.6	1.10, d (6.2)	21.0	1.20, d (6.4)
1-OH		9.32, s		9.36, s		8.65, s
3-OH		9.71, s		9.73, s		9.22, s
9-OH		4.75, d (5.0)				

[a] Measured at 600 (^{1}H) and 150 (^{13}C) MHz ([D_6]DMSO). [b] Measured at 400 (^{1}H) and 100 (^{13}C) MHz ([D_6]DMSO). [c] Overlapped with water peak. [d] Second order system.

ers above 3% population (Figure S2). H-9 and H-11 adopted *pseudo-axial* orientation in all conformers, in which the conformation of the fused heterocycle was practically the same and differed mainly in the arrangement of the hydroxyl and methoxyl groups. The Boltzmann-weighted TZVP ECD spectra (B3LYP, BH&HLYP, PBE0 functionals) of the conformers of the (9*R*,11*S*) enantiomer reproduced well the experimental ECD curve, with B3LYP giving the best agreement (Figure 4). Thus, the absolute configuration of **2** was determined as (+)-(9*R*,11*S*) and it was named xestodecalactone E. Apparently, the inversion of the C-9 chirality center did not have a significant effect on the ECD spectra.

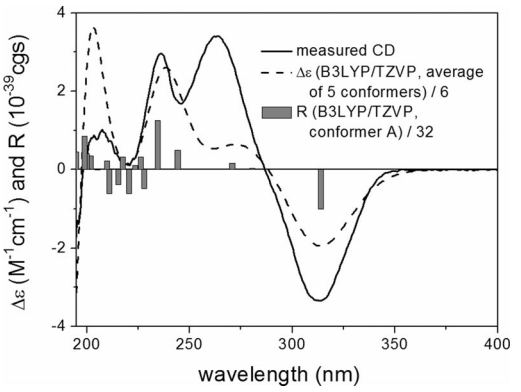

Figure 4. Experimental ECD spectrum of **2** in acetonitrile compared to the Boltzmann-weighted B3LYP/TZVP spectrum calculated for the five lowest-energy conformers of the truncated model of the (9*R*,11*S*)-enantiomer. Bars represent rotatory strength of the lowest-energy conformer.

Compound **3** was obtained as a yellowish amorphous mass. Its molecular formula was determined as $C_{19}H_{26}O_6$, on the basis of the $[M + Na]^+$ signal at *m/z* 373.1618 obtained by HRMS (ESI). ^{1}H NMR spectroscopic data of **3** (Table 1) showed familiar features to those observed for **1** and **2**, including one aromatic proton (δ_H = 6.14 ppm), a methoxyl group (δ_H = 3.66 ppm), two aromatic hydroxyl groups (δ_H = 8.65 and 9.22 ppm, assigned for 1- and 3-OH, respectively), a methylene group (δ_H = 3.29 and 3.76 ppm, CH_2-13), and signals attributed to the *n*-butyl side chain from CH_2-1′ (δ_H = 3.27 and 3.42 ppm) to CH_3-4′ (δ_H = 0.86 ppm). Inspection of the COSY correlations (Figure 1) confirmed the presence of the latter spin system, and showed the diagnostic homonuclear long-range correlation of CH_2-13 to H-4. They further revealed an additional continuous spin system from the olefinic CH-7 (δ_H = 6.18 ppm) to 11-CH_3 (δ_H = 1.20 ppm). By analogy to **1** and **2**, the HMBC experiment corroborated the attachment of the methoxyl group at C-2, the phenylacetic acid substructure of **3**, the ester bond linkage between C-12 (δ_C = 172.9 ppm) and the oxygenated methine group at C-11 (δ_H = 4.84 ppm), as well as the attachment of the *n*-butyl side chain to C-9 (δ_C = 79.9 ppm) through an ether linkage (Figure 2). Further inspection of the HMBC spectrum indicated correlations of CH-7 (δ_H = 6.18 ppm) with C-1, C-5, C-6 and C-8, CH-8 (δ_H = 5.46 ppm) with C-7 and C-9, CH-9 (δ_H = 3.84 ppm) with C-1′, C-7 and C-10, CH_2-10 (δ_H = 1.77 and 2.00 ppm) with C-8 and C-9, CH-11 (δ_H = 4.84 ppm) with

 © 0000 Wiley-VCH Verlag GmbH & Co. KGaA, Weinheim

C-9, and 11-CH_3 with C-10 and C-11. Accordingly, the fragment CH(7)CH(8)CH(9)CH_2(10)CH(11)CH_3 was established, indicating a possible reduction of the C-7–C-8 bond in **2** followed by dehydration at the same bond. Attachment to the aromatic ring at C-6 was deduced from correlations of CH-7 to C-6 and C-1 and C-5.

As with **1** and **2**, the relative configuration of **3** was determined from an analysis of the coupling constants and ROESY correlations. The axial orientations of protons H-9 and H-11 were evident from their large ^3J values ($^3J_{H-8ax,H-9ax}$ = 9.5 Hz, $^3J_{H-10ax,H-11ax}$ = 10.8 Hz). Moreover, H-9 showed a diagnostic through-space correlation with H-11, which is an indication of the *cis* orientation of H-9 and H-11 as found in **2**. In addition, the 1,3-*cis* diaxial relationship of H-9 and H-11 was found in all of the four computed low-energy conformers. The experimental ECD spectrum of **3** was completely different to those of **1** and **2** due to a different chromophore system. There were three negative CEs at 287, 250 and 216 nm and the 316 nm band was missing. The MMFF conformational search and DFT reoptimization of the 9-OMe model compound afforded four major conformers above 2% populations (see the Supporting Information, Figure S3). The Boltzmann-weighted ECD spectra of the (9*R*,11*S*) model compound showed good agreement with the experimental solution ECD curve (Figure 5), which proved that **3** is homochiral with **2**, i.e., it has (–)-(9*R*,11*S*) absolute configuration. Compound **3** was hence identified as a new natural product for which the name xestodecalactone F was proposed. The new optically active natural products **1**–**3** have the same (11*S*) absolute configuration, and their stereochemistry differed in the configuration of the C-9 chiral center. The ECD spectra of **1** and **2** are mirror images compared to those of the related xestodecalactones A–C, which confirms that the former belong to the (11*S*) series, whereas the latter belong to the (11*R*) series. A similar phenomenon has recently been found for curvularin derivatives; most curvularin-type natural products belong to the (15*S*) series, but (15*R*) derivatives have also been recently reported.[47,48]

Only **1** showed a *trans* configuration of H-9 and H-11, whereas **2** and **3** showed a *cis* relationship (Figure 6). However, the *cis*-isomer of **1** (**1a**) was also detected, albeit as a mixture with **1**. Upon measuring the ROESY spectrum of the mixture of both isomers, a clear cross-peak between H-9 and H-11 was observed only for the *cis* isomer **1a**. This

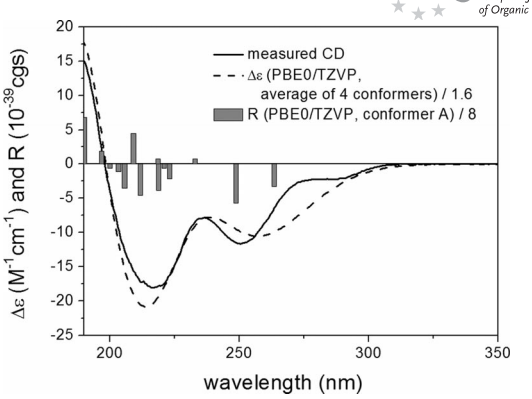

Figure 5. Experimental ECD spectrum of **3** in acetonitrile compared with the Boltzmann-weighted PBE0/TZVP spectrum calculated for the four lowest-energy conformers of the truncated model compound of the (9*R*,11*S*)-enantiomer. Bars represent rotatory strength of the lowest-energy conformer.

indicates the presence of both stereoisomers, as described previously for other derivatives,[44] however, the low amounts of the fraction available (ca. 0.9 mg) did not permit purification of the *cis* isomer **1a**.

Compound **4** was obtained as a grey amorphous powder with a molecular formula of $C_{15}H_{12}O_6$, deduced from the $[M + H]^+$ signal at *m/z* 289.0712 in the HRMS (ESI), thus revealing an increase in the molecular weight by 16 amu compared to the known corynesidone A (**5**), which was likewise isolated from *Corynespora cassiicola*.[41] The ^{1}H NMR spectra of both compounds were very similar, except for the presence of only one pair of *meta*-coupled protons in **4** (Table 2) instead of the two pairs in **5**. This was further confirmed by inspection of the COSY spectrum, which showed only one spin system composed of H-9, H-7 and CH_3-13. The aromatic proton appeared as a singlet at δ_H = 6.68 ppm (H-4) and showed a ω-correlation to the ester carbonyl group at δ_C = 163.6 ppm (C-11), and no correlation to the methyl group (CH_3-12, δ_H = 2.25 ppm, δ_C = 13.6 ppm) neither in the COSY nor in the HMBC spectra. On the other hand, the HMBC spectrum showed strong correlations (^3J) of both H-4 and CH_3-12 to C-11a (δ_C = 113.6 ppm) and the oxygenated C-2 (δ_C = 142.4 ppm). Thus, the 16 amu increase in molecular weight, corresponding to an additional oxygen atom in the structure of **4** compared to **5**, and the downfield chemical shift of C-2, re-

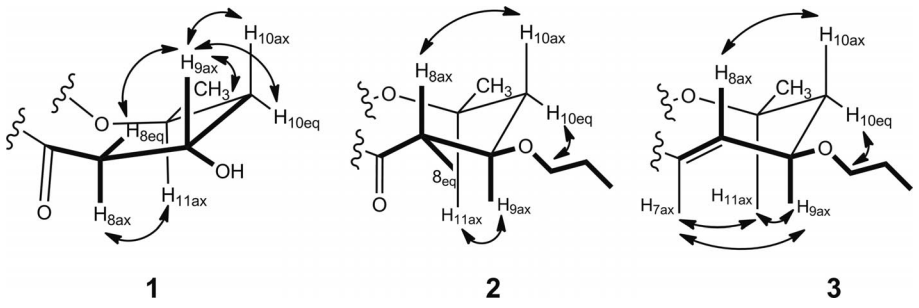

Figure 6. Key ROESY correlations of the new decalactones.

 © 0000 Wiley-VCH Verlag GmbH & Co. KGaA, Weinheim

vealed the presence of an additional hydroxyl group at C-2. Hence, **4** was identified as a new natural product and was given the name corynesidone D.

Table 2. NMR spectroscopic data of corynesidone D (**4**). Measured at 400 (^{1}H) and 100 (^{13}C) MHz ([D$_6$]acetone).

Position	**4** δ_C	δ_H	HMBC
1	128.6		
2	142.4		
3	150.5		
4	105.0	6.68, s	2, 3, 4a, 11, 11a
4a	156.6		
5a	143.8		
6	131.8		
7	114.2	6.45, d (2.0)	5a, 8, 9, 13
8	155.2		
9	105.7	6.45, d (2.0)	5a, 7, 8, 9a
9a	146.0		
11	163.6		
11a	113.6		
12	13.6	2.25, s	1, 2, 11a
13	16.0	2.26, s	5a, 6, 7

Compound **8** was obtained as a red-brown solid. MS and ^{1}H NMR (Table 3) data resembled those previously reported for 6-(3′-hydroxybutyl)-7-*O*-methylspinochrome B, isolated from *Fungi imperfecti*.[42] The structure was confirmed by inspection of COSY and HMBC spectra (Table 3). Although previously isolated, no attempts were made to determine the absolute stereochemistry of **8**. Hence, the modified Mosher procedure[49] was applied to determine the absolute configuration of the chiral center C-3′. The observed chemical shift differences (500 MHz, C_5D_5N) between the (2′*S*)-2′-methoxy-2′-trifluoromethyl-2′-phenylacetic acid (MTPA) ester and its (2′*R*)-MTPA diastereomer (Table 4) were consistent with the (3′*R*) absolute configuration of **8**.

The isolated compounds were subjected to a panel of bioassays to evaluate their potential activities. These included an estimation of their cytotoxic activity against murine L5178Y cells and antibacterial activity against multi drug resistant strains of *Staphylococcus aureus*, *Streptococcus pneumoniae*, *Enterococcus faecium*, and *Enterococcus cloacae*. In addition, antifungal activity of the isolated compounds against drug resistant strains of *Aspergillus fumigatus*, *Aspergillus faecalis*, *Candida albicans*, and *Candida krusei* was investigated, as well as their antitrypanosomal activity. None of the isolated natural products proved to be active in any of the cellular screens applied. However, in a biochemical protein kinase activity assay using 16 different human protein kinases, **6** and **8** inhibited several of the tested kinases (Table 5). The IC_{50} values observed for both compounds were in the low micromolar range against some protein kinases such as ALK, VEGF-R2, SRC, IGF1-R, and PIM1 of which inhibition is known to confer antitumoral effects. Of special interest is the fact that **6** inhibited PIM1with an IC_{50} value of 3.5×10^{-7} M, indicating a tenfold higher specificity of this naturally occurring inhibitor against this particular protein kinase in comparison to most of the other kinases investigated in this study (Table 5).

Table 3. NMR spectroscopic data of **8** at 600 (^{1}H) and 150 (^{13}C) MHz ([D$_6$]DMSO) and 6-(3′-hydroxybutyl)-7-*O*-methylspinochrome B (**8′**).

Position	**8** δ_C	δ_H	HMBC	**8′** δ_H
1	181.2			
2	161.1			
3	147.7			
4	185.7			
4a	105.8			
5	160.9			
6	122.3			
7	140.4			
8	107.3	7.04, s	6a, 7, 9, 10	7.06, s
8a	128.6			
1′	19.2	2.65, m	5, 6, 2′, 3′	2.65, t (6)
		2.63[a]	5, 6, 2′, 3′	2.65, t (6)
2′	38.9	1.51, m	1′, 3′,4′	1.50, m
		1.49, m	1′,3′,4′	1.50, m
3′	66.1	3.60, m	1′	3.50, m
4′	23.4	1.09, d (6.3)	2′, 3′	1.10, d (6)
7-OMe	60.3	3.78, s	7	3.85, s
OH-5		12.61, s	5, 6, 4a	12.65, s

[a] Overlapped by the solvent peak.

Table 4. Chemical shift difference between the (*S*)-MTPA and (*R*)-MTPA esters of **8**.

H atom	Chemical shift (δ_H, in C_5D_5N, at 500 MHz) 8	(*S*)-MTPA ester	(*R*)-MTPA ester	$\Delta\ \delta S - \delta R$
1′	3.31	2.27	2.33	–0.04
2′	2.16	1.61	1.90	–0.29
4′	1.40	1.30	1.28	+0.02

Table 5. IC_{50} values of compounds **6** and **8** against different protein kinases.[a].

	AKT1	ALK	ARK5	Aurora-B	AXL	FAK	IGF1-R	MEK1 wt
6	5.28E-05	4.26 E-06	4.92 E-05	1.57 E-06	9.13 E-06	2.21 E-05	4.87 E-06	> 1 E-04
8	7.18 E-05	5.65 E-06	6.96 E-05	2.83 E-05	9.15 E-06	1.73 E-05	3.51 E-06	> 1 E-04
	MET wt	NEK2	NEK6	PIM1	PLK1	PRK1	SRC	VEGF-R2
6	8.15 E-06	5.22 E-05	2.34 E-05	3.52 E-07	2.79 E-05	4.90 E-05	3.56 E-06	5.12 E-06
8	1.69 E-05	6.46 E-05	4.17 E-05	2.54 E-06	> 1 E-04	9.89 E-05	2.39 E-06	4.48 E-06

[a] Inhibitory potentials of compounds at various concentrations were determined in biochemical protein kinase activity assays. Listed are IC_{50} values in mol/L.

 © 0000 Wiley-VCH Verlag GmbH & Co. KGaA, Weinheim

Conclusion

The structures of three new xestodecalactones DˆF and a new corynesidone D have been determined through the use of 1D and 2D NMR spectroscopic techniques and mass analysis. Scheme 1 summarizes the deduced structures. ■■ ((<=Authors: this short conclusion has been added. Please check and extend if desired)) ■■

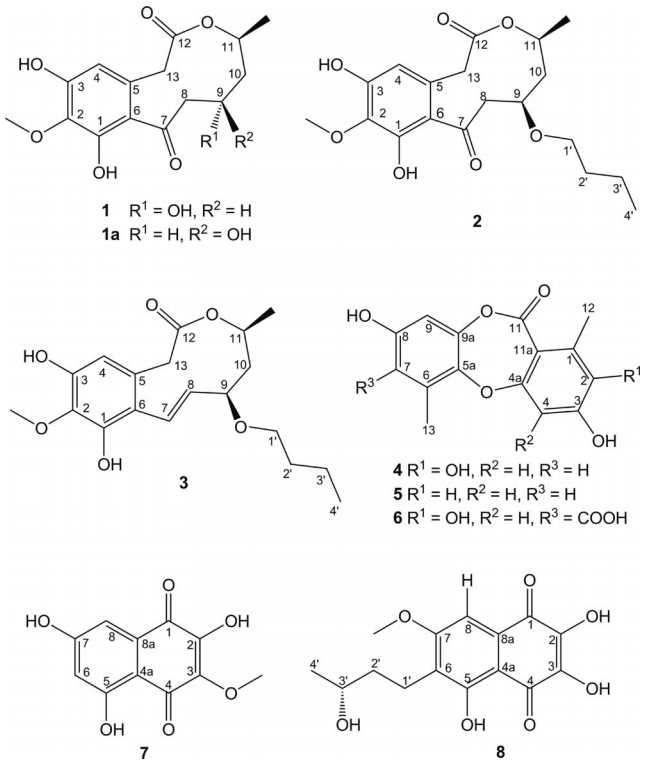

Scheme 1. Structures of isolated compounds.

Experimental Section

General Experimental Procedures: Optical rotation values were measured with a Perkin–Elmer-241 MC polarimeter. 1D and 2D NMR spectra were recorded with Bruker ARX 500, ARX 400, or AVANCE DMX 600 NMR spectrometers. MS (ESI) and HRMS (ESI) were obtained with Finnigan LCQ Deca and Micromass QTOF 2 mass spectrometers, respectively. Solvents were distilled prior to use, and spectral grade solvents were used for spectroscopic measurements. HPLC analysis was carried out with a Dionex P580 HPLC system coupled to a photodiode array detector (UVD340S). Routine detection was performed at 235, 254, 280, and 340 nm. The separation column (125 × 4 mm, L × i.d.) was prefilled with Eurospher-10 C_{18} (Knauer, Germany), and the following gradient was used (MeOH/0.02% H_3PO_4 in water); 0 min, 10% MeOH; 5 min, 10% MeOH; 35 min, 100% MeOH; 45 min, 100% MeOH.

Fungal Material: Fresh, healthy leaves of *Languncularia racemosa* (Combretacaeae) were collected in September 2009 from Hainan Island, China. Leaves were rinsed twice with sterilized distilled water. Surface sterilization was achieved by immersing the leaves in 70% ethanol for 2 min (twice) followed by rinsing twice in sterilized distilled water. The leaves were then cleaved aseptically into small segments (ca. 1 cm in length). The material was placed on a Petri dish (malt agar medium) containing an antibiotic to suppress bacterial growth (medium composition: 15 g/L malt extract, 15 g/L agar, and 0.2 g/L chloramphenicol in distilled water, pH 7.4–7.8) and incubated at room temperature (25 °C). After several days, hyphae growing from the plant material were transferred to fresh plates with the same medium, incubated again for 10 d, and periodically checked for culture purity.

Identification of Fungal Cultures: Fungal cultures were identified according to a molecular biological protocol by DNA amplification and sequencing of the ITS region as described previously.[50] The sequence data have been submitted to GenBank, accession number HQ389223. The fungal strain was identified as *Corynespora cassiicola*. A voucher strain (strain designation JCM 23.3) is kept in the Institute of Pharmaceutical Biology and Biotechnology, Düsseldorf, Germany.

Cultivation: Twenty Erlenmeyer flasks (1 L each) containing 100 g of rice and 100 mL of distilled water were autoclaved. A small part of the medium from a Petri dish containing the purified fungus was transferred under sterile conditions to the rice medium. The fungal strain was grown on solid rice medium at room temperature (22 °C) for 40 d.

Extraction and Fractionation: The culture was extracted extensively with EtOAc. The EtOAc extract was washed with water, taken to dryness, and partitioned between *n*-hexane and 90% MeOH. The 90% MeOH fraction was purified by chromatography over silica gel F_{254} (Merck, Darmstadt, Germany) using gradient elution (*n*-hexane/EtOAc/CH_2Cl_2/MeOH). One of the resulting fractions (MeOH/CH_2Cl_2, 60:40) was purified by chromatography over a Sephadex LH-20 column with 100% MeOH as solvent. Based on detection by TLC (silica gel F_{254}, Merck, Darmstadt, Germany) using EtOAc/MeOH/H_2O (77:13:10) as solvent system, collected fractions were combined and subjected to semipreparative HPLC (Merck, Hitachi L-7100) using a Eurosphere 100–10 C_{18} column (300 × 8 mm, L × i.d.) with the following gradient (MeOH/H_2O): 0 min, 10% MeOH; 5 min, 10% MeOH; 35 min 100% MeOH; 45 min, 100% MeOH. Yields of compounds were as follows: 2.1 mg (**1**), 2.2 mg (**2**), 2 mg (**3**), 3.4 mg (**4**), 2.2 mg (**5**), 19.4 mg (**6**), 1.8 mg (**7**), 49.2 mg (**8**).

Xestodecalactone D (1): Yield 2.1 mg; yellowish white amorphous powder; $[\alpha]_{20}^{D}$ = –25 (*c* 0.04, $CHCl_3$). UV (PDA): λ_{max} = 202.2, 222.5, 275.5 nm; ECD (CH_3CN, $c = 1.12 \times 10^{-3}$): λ_{max} ($\Delta\varepsilon$) = 316 (–3.73), 268 (3.31), 238 (3.19), 219 (–0.39), 207 (0.36), 192 (–4.11) nm; ^1H and ^{13}C in [D_6]DMSO, see Table 1. MS (ESI+): *m*/*z* = 311.0 $[M + H]^+$, 333.0 $[M + Na]^+$; MS (ESI–): *m*/*z* = 309.0 $[M - H]^-$; HRMS (ESI): calcd. for $C_{15}H_{19}O_7$ $[M + H]^+$ 311.1131; found 311.1134.

Xestodecalactone E (2): Yield 2.2 mg; yellowish amorphous mass; $[\alpha]_{20}^{D}$ = +12 (*c* = 0.115, $CHCl_3$); UV (PDA): λ_{max} = 220.9, 252.5 nm; ECD (CH_3CN, $c = 2.05 \times 10^{-3}$): λ_{max} ($\Delta\varepsilon$) = 313 (–3.34), 264 (3.41), 236 (2.96), 207 (1.03), 192 (–3.05) nm; ^1H and ^{13}C in [D_6]DMSO, see Table 1. MS (ESI+): *m*/*z* = 366.9 $[M + H]^+$, 754.7 $[2M + Na]^+$; MS (ESI–): *m*/*z* = 365.0 $[M - H]^-$; HRMS (ESI): calcd. for $C_{19}H_{26}O_7$ $[M + H]^+$ 367.1751; found 367.1752.

Xestodecalactone F (3): Yield 2.0 mg; yellowish amorphous mass; $[\alpha]_{20}^{D}$ = –180 (*c* = 0.04, $CHCl_3$). UV (PDA): λ_{max} = 202.8, 221.8, 274.8 nm; ECD (CH_3CN, $c = 0.85 \times 10^{-3}$): λ_{max} ($\Delta\varepsilon$) = 287 (sh, –2.23), 250 (–11.65), 216 (–18.09), positive below 198 nm. ^1H and ^{13}C in [D_6]DMSO, see Table 1. MS (ESI+): *m*/*z* = 722.0 $[2M + Na]^+$; MS (ESI–): *m*/*z* = 349.0 $[M - H]^-$; HRMS (ESI): calcd. for $C_{19}H_{26}O_6$ $[M + Na]^+$ 373.1627; found 373.1618.

Corynesidone D (4): Yield 3.4 mg; grey amorphous powder; UV (PDA): λ_{max} = 230.7, 271.7 nm; ^1H and ^{13}C in [D_6]acetone, see

 © 0000 Wiley-VCH Verlag GmbH & Co. KGaA, Weinheim

Table 2. MS (ESI+): m/z = 289.1 $[M + H]^+$, 598.8 $[2M + Na]^+$, 886.5 $[3M + Na]^+$; MS (ESI–): m/z = 287.1 $[M – H]^–$; HRMS (ESI): calcd. for $C_{15}H_{13}O_6$ $[M + H]^+$ 289.0712; found 289.0712.

6-(3′-Hydroxybutyl)-7-*O*-methylspinochrome B (8): Yield 49.2 mg; red-brown solid; $[\alpha]^D_{20}$ = –12 (c = 0.025, acetone); UV (PDA) λ_{max} = 213.7, 268.0, 320.7 nm; ^1H and ^{13}C in $[D_6]$DMSO (Table 3), MS (ESI+): m/z = 309.1 $[M + H]^+$, 331.0 $[M + Na]^+$; MS (ESI–): m/z = 307.1 $[M – H]^–$.

Mosher Method: The reaction was performed according to a convenient Mosher ester procedure.[49]

Biochemical Protein Kinase Activity Assay: Protein kinase inhibitory activity was determined in 96-well plates as described previously.[51] The following substrates were used: GSK3(14–27), AKT1, NEK6, PIM1; tetra(LRRWSLG), Aurora B; poly(Glu,Tyr)$_{4:1}$, FAK, IGF1-R, SRC, VEGF-R2; poly(Ala,Glu,Lys,Tyr)$_{6:2:5:1}$, ALK, AXL, METwt; ERK2-KR, MEK1 wt; Rb-CTF, NEK2; RBER-CHKtide, PLK1, PRK1. Autophosphorylation was measured for ARK5.

Computational Section: Conformational searches were carried out by using Macromodel 9.7.211[52] software employing the Merck Molecular Force Field (MMFF) with implicit solvent model for chloroform. Geometry reoptimizations at the B3LYP/6-31G(d) level of theory followed by TDDFT calculations using various functionals (B3LYP, BH&HLYP, PBE0) and TZVP basis set were performed by the Gaussian 03[53] package. Boltzmann distributions were estimated from the ZPVE corrected B3LYP/6-31G(d) energies. ECD spectra were generated as the sum of Gaussians[54] with 3000 and 2100 cm^{-1} half-height width (corresponding to ca. 19 and 13 nm at 250 nm, respectively), using dipole-velocity computed rotational strengths for conformers above 3%. The MOLEKEL[55] software package was used for visualization of the results.

Acknowledgments

This project was supported by grants from the Bundesministerium für Bildung und Forschung (BMBF) to P. P., A. D., and M. K., and from the Ministry of Science and Technology of China (MOST) to W. L. We are indebted to C. Kakoschke for NMR measurements (HZI, Braunschweig, Germany). T. K. thanks the New Hungary Development Plan, cofinanced by the European Social Fund and the European Regional Development Fund (TÁMOP 4.2.1./B-09/1/KONV-2010-0007). A scholarship (grant number 10/6/117) granted and financed by the Egyptian Government, Ministry of High Education to W. E. is gratefully acknowledged.

[1] A. H. Aly, A. Debbab, J. Kjer, P. Proksch, *Fungal Divers.* **2010**, *41*, 1–16.
[2] A. Debbab, A. H. Aly, W. Lin, P. Proksch, *Microbial Biotechnol.* **2010**, *3*, 544–563.
[3] A. H. Aly, A. Debbab, P. Proksch, *Appl. Microbiol. Biotechnol.* **2011**, *90*, 1829–1845.
[4] A. Debbab, A. H. Aly, P. Proksch, *Fungal Divers.* **2011**, *49*, 1–12.
[5] A. H. Aly, A. Debbab, P. Proksch, *Fungal Divers.* **2011**, *50*, 3–19.
[6] G. A. Strobel, R. V. Miller, C. Miller, M. Condron, D. B. Teplow, W. M. Hess, *Microbiology* **1999**, *45*, 1919–1926.
[7] S. B. Singh, D. L. Zink, Z. Guan, J. Collado, F. Pelaez, P. J. Felock, D. J. Hazuda, *Helv. Chim. Acta* **2003**, *86*, 3380–3385.
[8] Y. M. Ma, Y. Li, J. Y. Liu, Y. C. Song, R. X. Tan, *Fitoterapia* **2004**, *75*, 451–456.
[9] A. Stierle, G. Strobel, *J. Nat. Prod.* **1995**, *58*, 1315–1324.
[10] G. A. Strobel, X. Yang, J. Sears, R. Kramer, R. S. Sidhu, W. M. Hess, *Microbiology* **1993**, *142*, 435–440.
[11] G. Vassal, C. Pondarré, I. Boland, C. Cappelli, A. Santos, C. Thomas, E. Lucchi, K. Pein, F. Imadalou, J. Morizet, A. Gouyette, *Biochimie Mar.* **1998**, *80*, 271–80.
[12] A. L. Eyberger, R. Dondapati, J. R. Porter, *J. Nat. Prod.* **2006**, *69*, 1121–1124.
[13] V. Kumaresan, T. S. Suryanarayanan, *Mycol. Res.* **2001**, *105*, 1388–1391.
[14] E. B. Gareth Jones, S. J. Stanley, U. Pinruan, *Botanica Marina* **2008**, *51*, 163–170.
[15] T. Takemura, N. Hanagata, K. Sugihara, S. Baba, I. Karube, Z. Dubinsky, *Aquat. Bot.* **2000**, *68*, 15–28.
[16] A. K. Parida, A. B. Das, *Ecotoxicol. Environ. Saf.* **2005**, *60*, 324–349.
[17] E. L. Gilman, J. Ellison, N. C. Duke, C. Field, *Aquat. Bot.* **2008**, *89*, 237–250.
[18] Z.-S. Cheng, J. Pan, W. Tang, Q. Chen, Y. Lin, *J. For. Res.* **2009**, *20*, 63–72.
[19] F. Waller, B. Achatz, H. Baltruschat, J. Fodor, K. Becker, M. Fischer, T. Heier, R. Hückelhoven, C. Neumann, D. von Wettstein, P. Franken, K. H. Kogel, *Proc. Natl. Acad. Sci. USA* **2005**, *102*, 13386–13391.
[20] H. W. Zhang, Y. C. Song, R. X. Tan, *Nat. Prod. Rep.* **2006**, *23*, 753–771.
[21] J. W. Blunt, B. R. Copp, M. H. G. Munro, P. T. Northcote, M. R. Prinsep, *Nat. Prod. Rep.* **2010**, *27*, 165–237.
[22] B. J. Rawlings, *Nat. Prod. Rep.* **1999**, *16*, 425–484.
[23] J. Kobayashi, T. Kubota, *J. Nat. Prod.* **2007**, *70*, 451–460.
[24] P. M. Dewick, *Medicinal natural products: a biosynthetic approach*, John Wiley & Sons, **2002**, Chichester, UK, p. 35.
[25] R. G. Coombe, J. J. Jacobs, T. R. Watson, *Aust. J. Chem.* **1968**, *21*, 783–788.
[26] D. J. Robeson, G. A. Strobel, *Z. Naturforsch. C* **1981**, *36*, 1081–1083.
[27] S. Lai, Y. Shizuri, S. Yamamura, K. Kawai, Y. Terada, H. Furukawa, *Tetrahedron Lett.* **1989**, *30*, 2241–2244.
[28] A. J. Birch, O. C. Musgrave, R. W. Rickards, H. Smith, *J. Chem. Soc.* **1959**, *4*, 3146–3152.
[29] Y. Liu, Z. Li, J. C. Vederas, *Tetrahedron* **1998**, *54*, 15937–15958.
[30] A. H. Aly, A. Debbab, R. A. Edrada-Ebel, W. E. G. Müller, M. H. G. Kubbutat, V. Wray, R. Ebel, P. Proksch, *Mycosphere* **2010**, *1*, 153–162.
[31] J. Xu, A. Aly, V. Wray, P. Proksch, *Tetrahedron Lett.* **2011**, *52*, 21–25.
[32] A. Debbab, A. H. Aly, R. Edrada-Ebel, V. Wray, W. E. Mueller, F. Totzke, U. Zirrgiebel, C. Schaechtele, M. H. Kubbutat, W. H. Lin, M. Mosaddak, A. Hakiki, P. Proksch, R. Ebel, *J. Nat. Prod.* **2009**, *72*, 626–631.
[33] A. Debbab, A. H. Aly, R. Edrada-Ebel, V. Wray, A. Pretsch, G. Pescitelli, T. Kurtan, P. Proksch, *Eur. J. Org. Chem.* **2012**, *7*, 1351–1359.
[34] L. Yánez-Espinosa, T. Terrazas, L. López-Mata, J. I. Valdez-Hernández, *Wood Sci. Technol.* **2004**, *38*, 217–226.
[35] W. M. Bandaranayake, *Mangrove Salt Marsh.* **1998**, *2*, 133–148.
[36] P. H. List, L. Horhammer, ######### ? #########, Springer, Berlin, **1969–1970**, vol. 2–6 ■■ ((<=Author: please add the book title)) ■■ .
[37] J. F. Morton, *Econ. Bot.* **1965**, *19*, 113–123.
[38] W. A. Collier, T. Tjong, A. Hung, *Rev. Med. Vet. Parasitol.* **1952**, *11*, 11–30.
[39] P. A. Paranagama, E. M. K. Wijeratne, A. M. Burns, M. T. Marron, M. K. Gunatilaka, A. E. Arnold, A. A. L. Gunatilaka, *J. Nat. Prod.* **2007**, *70*, 1700–1705.
[40] E. M. K. Wijeratne, B. P. Bashyal, M. K. Gunatilaka, A. E. Arnold, A. A. L. Gunatilaka, *J. Nat. Prod.* **2010**, *73*, 1156–1159.
[41] P. Chomcheon, S. Wiyakrutta, N. Sriubolmas, N. Ngamrojanavanich, S. Kengtong, C. Mahidol, S. Ruchirawat, P. Kittakoop, *Phytochemistry* **2009**, *70*, 407–413.

 © 0000 Wiley-VCH Verlag GmbH & Co. KGaA, Weinheim

[42] H. Chimura, T. Sawa, Y. Kumada, F. Nakamura, M. Matsuzaki, *J. Antibiot.* **1973**, *26*, 618–20.
[43] G. Assante, R. Locci, L. Camarda, L. Merlint, G. Nasini, *Phytochemistry* **1977**, *16*, 243–247.
[44] R. Edrada, M. Heubes, G. Brauers, V. Wray, A. Berg, U. Berg, M. Wohlfarth, J. Muehlbacher, K. Schaumann, S. G. Bringmann, P. Proksch, *J. Nat. Prod.* **2002**, *65*, 1598–1604.
[45] Y.-S. Cai, T. Kurtán, Z.-H. Miao, A. Mándi, I. Komáromi, H.-L. Liu, J. Ding, Y.-W. Guo, *J. Org. Chem.* **2011**, *76*, 1821–1830.
[46] Y. Zhou, A. Mándi, A. Debbab, V. Wray, B. Schulz, W. E. G. Müller, W. H. Lin, P. Proksch, T. Kurtán, A. H. Aly, *Eur. J. Org. Chem.* **2011**, 6009–6019.
[47] H. Greve, P. J. Schupp, E. Eguereva, S. Kehraus, G. Kelter, A. Maier, H. H. Fiebig, G. M. König, *Eur. J. Org. Chem.* **2008**, 5085–5092.
[48] J. Dai, K. Krohn, U. Flörke, G. Pescitelli, G. Kerti, T. Papp, K. E. Kövér, A. C. Bényei, S. Draeger, B. Schulz, T. Kurtán, *Eur. J. Org. Chem.* **2010**, 6928–6937.
[49] B. N. Su, E. J. Park, Z. H. Mbwambo, B. D. Santarsiero, A. D. Mesecar, H. H. S. Fong, J. M. Pezzuto, A. D. Kinghorn, *J. Nat. Prod.* **2002**, *65*, 1278–1282.
[50] S. Wang, X. M. Li, F. Teuscher, D. L. Li, A. Diesel, R. Ebel, P. Proksch, B. G. Wang, *J. Nat. Prod.* **2006**, *69*, 1622–1625.
[51] A. H. Aly, R. A. Edrada-Ebel, I. D. Indriani, V. Wray, W. E. G. Müller, F. Zirrgiebel, U. Totzke, C. Schaechtele, M. H. G. Kubbutat, W. H. Lin, P. Proksch, R. Ebel, *J. Nat. Prod.* **2008**, *71*, 972–980.
[52] MacroModel, Schrödinger LLC, **2009**; http://www.schrodinger.com.
[53] M. J. Frisch, G. W. Trucks, H. B. Schlegel, G. E. Scuseria, M. A. Robb, J. R. Cheeseman, J. A. Montgomery Jr, T. Vreven, K. N. Kudin, J. C. Burant, J. M. Millam, S. S. Iyengar, J. Tomasi, V. Barone, B. Mennucci, M. Cossi, G. Scalmani, N. Rega, G. A. Petersson, H. Nakatsuji, M. Hada, M. Ehara, K. Toyota, R. Fukuda, J. Hasegawa, M. Ishida, T. Nakajima, Y. Honda, O. Kitao, H. Nakai, M. Klene, X. Li, J. E. Knox, H. P. Hratchian, J. B. Cross, V. Bakken, C. Adamo, J. Jaramillo, R. Gomperts, R. E. Stratmann, O. Yazyev, A. J. Austin, R. Cammi, C. Pomelli, J. W. Ochterski, P. Y. Ayala, K. Morokuma, G. A. Voth, P. Salvador, J. J. Dannenberg, V. G. Zakrzewski, S. Dapprich, A. D. Daniels, M. C. Strain, O. Farkas, D. K. Malick, A. D. Rabuck, K. Raghavachari, J. B. Foresman, J. V. Ortiz, Q. Cui, A. G. Baboul, S. Clifford, J. Cioslowski, B. B. Stefanov, G. Liu, A. Liashenko, P. Piskorz, I. Komaromi, R. L. Martin, D. J. Fox, T. Keith, M. A. Al-Laham, C. Y. Peng, A. Nanayakkara, M. Challacombe, P. M. W. Gill, B. Johnson, W. Chen, M. W. Wong, C. Gonzalez, J. A. Pople, *Gaussian 03*, revision C.02, Gaussian, Inc., Wallingford CT, **2004**.
[54] P. J. Stephens, N. Harada, *Chirality* **2010**, *22*, 229–233.
[55] U. Varetto, *MOLEKEL*, v.5.4, Swiss National Supercomputing Centre, Manno, Switzerland, **2009**.

Received: March 2, 2012

 © 0000 Wiley-VCH Verlag GmbH & Co. KGaA, Weinheim

Natural Products

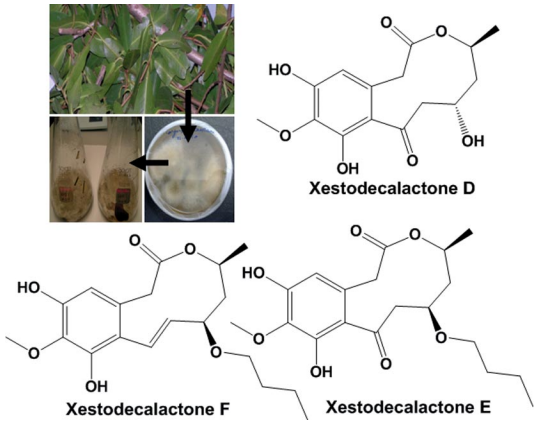

Three new xestodecalactones D˜F (**1**–**3**) and a new corynesidone D were isolated from *Corynespora cassiicola*. The structures were determined by 1D and 2D NMR spectroscopy as well as by high-resolution mass spectrometry. The absolute configurations of **1**–**3** were determined by TDDFT ECD calculations. All compounds were tested against a panel of human protein kinases.

W. Ebrahim, A. H. Aly, A. Mándi, F. Totzke, M. H. G. Kubbutat, V. Wray, W. Lin, H. Dai, P. Proksch, T. Kurtán,* A. Debbab*

Decalactone Derivatives from *Corynespora cassiicola*, an Endophytic Fungus of the Mangrove Plant *Laguncularia racemosa*

Keywords: Natural products / Medicinal chemistry / Drug discovery / Fungi / Structure elucidation / Conformation analysis / Lactones

 © 0000 Wiley-VCH Verlag GmbH & Co. KGaA, Weinheim